

Gold-Graphene PCF-SPR Sensor with ML for Advanced Optical Properties Prediction

Major Project Report

*Provided in partial satisfaction of the prerequisites for the
degree of*

**BACHELOR OF TECHNOLOGY
in
ELECTRONICS AND COMMUNICATION ENGINEERING**

by

Rajwardhan Patil AND Gaurav Raj
Roll No.211EC134
Roll No. 211EC114

Under the guidance of

B.Nagavel



DEPARTMENT OF ELECTRONICS AND COMMUNICATION
ENGINEERING
NATIONAL INSTITUTE OF TECHNOLOGY, KARNATAKA
SURATHKAL, MANGALORE - 575025

MAY, 2025

DECLARATION

written by Rajwardhan Patil And Gaurav Raj

I hereby declare that the Major project entitled "**Gold-Graphene PCF-SPR Sensor with ML for Advanced Optical Properties Prediction**", which is being submitted to the National Institute of Technology Karnataka,Surathkal in partial fulfilment of the requirements for the award of the Degree of Bachelor of Technology in EC Engineering is a Bonafide report of the project work carried out by us. The material contained in this project report has not been submitted to any University or Institution for the award of any degree.

Rajwardhan Patil — Gaurav Raj

Roll no.:211EC134

Roll no.:211EC114

Department of Electronics and Communication Engineering

Place: NITK, Surathkal

Date: May, 2025

CERTIFICATE

This is to certify that the major project entitled "**Gold-Graphene PCF-SPR Sensor with ML for Advanced Optical Properties Prediction**", submitted by Rajwardhan Patil and Rajwardhan Patil (Roll No: 21IEC134, 21IEC114) as the record of the project work carried out by them, is accepted as the evaluation report submission in partial fulfilment of the requirements for the award of degree of Bachelor of Technology in Electronics and Communications Engineering.



6/5/25

B. Nagavel
Project Guide Professor
Dept. of ECE
NITK Surathkal - 575025

ACKNOWLEDGEMENT

We wish to express our profound gratitude and indebtedness to B. Nagavel, who guided us throughout this fascinating project on the topic "**Gold-Graphene PCF-SPR Sensor with ML for Advanced Optical Properties Prediction**". We find words inadequate to thank him for his encouragement and valuable suggestions during this work. We are also grateful to all faculty members and staff who have supported us. We acknowledge our indebtedness to all those whose work has been referenced in the understanding and completion of this project. We also thank all our well-wishers who have patiently extended all sorts of help and moral support for accomplishing this dissertation.

Rajwardhan Patil

Gaurav Raj

Date: 6/5/2025

ABSTRACT

This project focuses on the development of a gold-coated PCF-SPR sensor, with graphene used as the binding material to enhance the sensor's sensitivity and overall performance. The gold layer enhances plasmonic resonance, improving light interaction with the analyte, while graphene is applied as the binding material to increase the sensor's surface area and conductivity, contributing to better performance in detecting small changes in the refractive index (RI) of analytes.

By adjusting key parameters such as pitch (the distance between the centers of adjacent holes) and hole diameter, the sensor's performance is optimized. These parameters are critical in determining the sensor's ability to propagate light effectively and interact with the analyte. The right combination of these values improves the sensor's wavelength sensitivity, amplitude sensitivity, and confinement loss.

Further adjustments were made by varying graphene thickness and gold layer thickness. These parameters were fine-tuned to improve plasmonic resonance and enhance the sensor's sensitivity by maximizing light absorption and interaction at the sensor-analyte interface.

The machine learning component of this project further boosts the sensor's predictive power by modeling complex relationships between various sensor parameters and the observed optical properties. A series of experiments and simulations were conducted to validate the sensor's performance, demonstrating a maximum wavelength sensitivity of 12000 nm/RIU and a maximum amplitude sensitivity of -1077.83 RIU⁻¹ with a corresponding resolution value of 8.3E-07 RIU.

The proposed gold-coated PCF-SPR sensor, when integrated with ML algorithms, offers a promising solution for highly sensitive and accurate detection in a range of applications, including environmental monitoring, biological sensing, and chemical analysis. Future work will focus on further optimizing the sensor structure and incorporating real-time data processing for practical deployment in industrial and research settings.

Contents

1	Introduction	1
1.1	Overview	1
1.2	Problem Statement	1
1.3	Motivation	2
1.4	Objectives of the Research	2
2	Literature Survey	4
2.1	Overview	4
3	Theoretical Background	6
3.1	Introduction to SPR Sensors	6
3.2	Limitations of Traditional SPR Sensors	6
3.3	Existing SPR Sensor Designs	7
3.4	Material Innovations in SPR Sensors	8
3.5	Advances in Simulation and Optimization	9
4	Simulation Results and Discussions	10
4.1	Problem Formulation and System Model	10
4.2	Design Exploration and Simulation Process	12
4.3	Results	16
5	Conclusion	24
6	References	26

List of Figures

4.1	PCF-SFR sensor model	10
4.2	X-polarized Core Mode: The electric field is concentrated symmetrically around the core region, with peak intensity at the center. The magnetic field vectors (red arrows) indicate transverse magnetic field oscillations aligned with the x-axis. This mode exhibits strong confinement within the core, leading to high mode purity.	11
4.3	Y-polarized Core Mode: The field distribution is again centered in the core, but polarized along the y-direction. The red magnetic vectors are now aligned accordingly, indicating orthogonal polarization compared to the first mode. This mode is essential for analyzing birefringence and polarization sensitivity.	12
4.4	Surface Plasmon Polariton (SPP) Mode: Unlike the core modes, the electric field is now highly localized at the metal-dielectric interface, indicating the excitation of surface plasmons. The magnetic field vectors are oriented perpendicular to the interface, confirming the SPP nature. This mode exhibits strong field enhancement near the sensor surface, making it highly sensitive to refractive index variations.	12
4.5	(Left) Confinement loss for different graphene thickness values and analyte refractive indices; (Right) Confinement loss for varying gold layer thickness values and corresponding wavelength shifts.	17
4.6	(Left) Confinement loss for varying hole diameters and analyte refractive indices; (Right) Confinement loss for varying pitch values and wavelength shifts.	18
4.7	(Left) KNNR: Predicted vs Actual n_{eff} ; (Right) KNNR: Predicted vs Actual Core Loss	19
4.8	(Left) DecisionTree: Predicted vs Actual n_{eff} ; (Right) DecisionTree: Predicted vs Actual Core Loss	20
4.9	(Left) RFR: Predicted vs Actual n_{eff} ; (Right) RFR: Predicted vs Actual Core Loss	20
4.10	(Left) Correlation Matrix Heatmap of various parameters; (Right) Training and validation with three layers	21
4.11	(Left) MSE vs Epochs for training and validation; (Right) KNNR: Predicted vs Actual n_{eff} and Core Loss	21
4.12	(Left) DecisionTree: Predicted vs Actual n_{eff} and Core Loss; (Right) RFR: Predicted vs Actual n_{eff} and Core Loss	22
4.13	Performance metrics for varying analyte refractive index values, showing amplitude sensitivity, wavelength sensitivity, and resolution. . .	22

Chapter 1

Introduction

1.1 Overview

This project focuses on improving the performance of Surface Plasmon Resonance (SPR) sensors, which are widely used for detecting small changes in the refractive index in various fields like biomedical diagnostics, environmental monitoring, and chemical sensing. Traditional SPR sensors face challenges such as limited sensitivity, scalability, and computational inefficiency when used in complex or dynamic environments.

To address these challenges, the project proposes a new SPR sensor design with a dual-metal layer coating of gold and graphene on a single-core Photonic Crystal Fiber (PCF). This new design aims to enhance the sensor's sensitivity and overall performance. By optimizing key parameters like the analyte refractive index, hole diameter, and metal layer thickness through simulations in COMSOL Multiphysics, the sensor design is fine-tuned to achieve better results.

In addition, machine learning techniques are applied to predict and optimize key performance metrics such as configuration loss and the effective refractive index n_{eff} .

This integration of simulations and machine learning ensures the sensor's design is efficient and meets the required performance standards. The overall goal of this project is to create a more sensitive, efficient, and scalable SPR sensor suitable for real-time applications in various industries.

1.2 Problem Statement

This project aims to design a novel SPR sensor with a gold-metal coating and graphene used as the binding material on a single-core Photonic Crystal Fiber (PCF). The gold layer is chosen for its plasmonic properties, enhancing the interaction of light with the analyte, while graphene serves as the binding material to improve the sensor's surface area and conductivity, further enhancing its sensitivity and overall performance. The goal is to enhance the sensor's sensitivity and performance. Additionally, machine learning techniques will be employed to predict and optimize key performance metrics, ensuring the sensor meets the necessary standards for real-world applications.

1.3 Motivation

The development of highly sensitive and efficient sensors is crucial in today's rapidly evolving technological landscape, particularly in fields like biomedical diagnostics, environmental monitoring, and chemical sensing. Surface Plasmon Resonance (SPR) sensors have proven to be invaluable tools for detecting small changes in refractive index, which makes them suitable for applications that require real-time, high-accuracy data. However, conventional SPR sensors face limitations in sensitivity, scalability, and computational efficiency, which restricts their widespread application in complex, dynamic environments.

Addressing these challenges is the primary motivation behind this project. The potential to improve SPR sensor performance and make them more reliable for real-time applications is what drives this research. By incorporating innovative materials such as graphene alongside gold in the sensor's design, the project seeks to unlock greater sensitivity and improved signal stability, essential for a wide range of industries.

Moreover, leveraging machine learning for optimizing performance metrics such as configuration loss and the effective refractive index n_{eff} offers a unique opportunity to enhance sensor accuracy and reliability, further advancing the field of SPR sensing technology. This project aims to create a more scalable and efficient SPR sensor that can meet the growing demands for high-performance sensors in diverse, real-world scenarios, ultimately contributing to advancements in healthcare, environmental science, and industrial monitoring.

1.4 Objectives of the Research

The primary objective of this research is to design a novel Surface Plasmon Resonance (SPR) sensor using a dual-metal layer coating of gold and graphene on a single-core Photonic Crystal Fiber (PCF). This design aims to improve the sensor's sensitivity and overall performance, addressing the limitations of conventional SPR sensors.

Additionally, the research aims to optimize key design parameters, including the analyte refractive index, hole diameter, and the thickness of the metal layers. These optimizations will be performed through simulations in COMSOL Multiphysics to fine-tune the sensor's performance and ensure better sensitivity and efficiency. The study offers two novel approaches to maximize the IRS phase shifts. Large reflecting array deployment is made easier by these approaches, which are intended to lower the overhead associated with channel estimation. Robust communication in vehicle networks is dependent on these arrangements.

Another key objective is to integrate machine learning techniques to predict and optimize critical performance metrics, such as configuration loss and the effective refractive index n_{eff} . This will help ensure that the sensor design meets the desired performance standards.

The research also focuses on creating a highly sensitive, efficient, and scalable SPR sensor that can be applied to real-time applications across various industries, such as biomedical diagnostics, environmental monitoring, and chemical sensing.

Finally, the research aims to validate the sensor's performance through simulations and optimizations, ensuring that it is suitable for large-scale, real-time applications..

Chapter 2

Literature Survey

2.1 Overview

Surface Plasmon Resonance (SPR) sensors are critical for detecting refractive index changes in applications like biomedical diagnostics, environmental monitoring, and chemical sensing. However, traditional SPR sensors face limitations in sensitivity, scalability, and computational efficiency. This review focuses on single-core, double-core, and multi-analyte structures, as well as recent advances in material selection and optimization techniques.

Single-Core and Double-Core SPR Sensors

- Single-Core SPR Sensors: Simple and cost-effective, but with limited sensitivity, especially for low-concentration analytes in complex environments.
- Double-Core SPR Sensors: Offer enhanced sensitivity by improving light interaction, but they are more complex and costly to fabricate.

Our research integrates insights from these designs and proposes a single-core PCF SPR sensor with dual-metal layer coatings (gold and graphene), combining high sensitivity with easier fabrication.

While not extensively studied, we explored the concept of multi-analyte SPR sensors, which have the ability to detect multiple substances simultaneously. These sensors are highly versatile, particularly in applications requiring the detection of various analytes at once. However, the challenges of scalability and data processing have limited the broader adoption of these sensors. Multi-analyte sensors could offer significant advantages in fields like biomedical diagnostics and environmental monitoring, where simultaneous detection of multiple substances is often necessary, but their current limitations in handling large datasets and scaling for real-world applications remain an obstacle.

Recent research has focused on material innovations to improve the sensitivity and stability of SPR sensors, with particular attention given to the combination of gold and graphene. Gold enhances the plasmonic resonance necessary for effective SPR sensing, while graphene contributes a high surface area and exceptional conductivity. This combination of materials not only improves the overall performance of SPR sensors but also enhances their robustness in challenging environments. These innovations in material selection are key to advancing the effectiveness of SPR sensors, allowing for more reliable and accurate detection. This work is reflected in the research conducted by Kumar et al. [1] and Saha et al. [2], which

demonstrated how material advancements have led to improvements in sensor sensitivity.

Furthermore, the design of SPR sensors has been significantly enhanced through simulation and optimization techniques. Tools like COMSOL Multiphysics allow for precise simulation of sensor parameters, including analyte refractive index, hole diameter, and metal layer thickness. These simulations help in fine-tuning the sensor design for optimal performance. Additionally, the integration of machine learning techniques has become increasingly valuable in predicting key performance metrics such as configuration loss and effective refractive index n_{eff} , enabling more efficient sensor optimization. The work by Hasan et al. [4] utilizes machine learning models such as Random Forest Regression (RFR) to predict critical sensor parameters and improve the overall performance of SPR sensors.

Despite these advancements, many SPR sensors still face challenges related to sensitivity and efficiency. Multi-analyte sensors, though promising, are not yet scalable for large-scale use. This research aims to address these gaps by combining single-core designs, dual-metal coatings, and machine learning to create a more sensitive, efficient, and scalable SPR sensor for real-world applications.

Chapter 3

Theoretical Background

3.1 Introduction to SPR Sensors

Surface Plasmon Resonance (SPR) is a widely used optical technique for detecting changes in the refractive index at the surface of a sensor, making it an invaluable tool in various scientific and industrial fields. SPR sensors operate on the principle of exciting surface plasmon waves at the interface of a metal and dielectric medium. When light strikes the metal surface at a specific angle, the surface plasmons are excited, and any change in the refractive index near the surface leads to a shift in the resonance angle, which can be measured. This shift provides real-time information about changes in the environment surrounding the sensor.

SPR sensors have numerous applications in fields like biomedical diagnostics, environmental monitoring, and chemical sensing. They are particularly useful for detecting the presence of biomolecules, pollutants, or chemical substances with high precision. These sensors offer non-invasive, label-free detection and can operate in real-time, making them ideal for applications requiring continuous monitoring or rapid detection.

Despite their advantages, traditional SPR sensors face limitations, particularly when it comes to sensitivity, scalability, and efficiency. Traditional SPR designs, while effective, often struggle to detect low-concentration analytes in complex environments, and they can be expensive and difficult to scale for widespread use. Additionally, the complexity of their fabrication processes further restricts their deployment in practical, large-scale applications.

Recent advancements in SPR sensor technology have focused on improving sensitivity and scalability through innovations such as Photonic Crystal Fibers (PCF) and the use of advanced materials like graphene. These developments aim to overcome the limitations of traditional SPR sensors, making them more sensitive, efficient, and cost-effective for a broader range of real-world applications.

3.2 Limitations of Traditional SPR Sensors

Traditional SPR sensors have several limitations that affect their performance and scalability in real-world applications:

1. Limited Sensitivity: Traditional SPR sensors, especially single-core designs, struggle to detect low-concentration analytes, particularly in complex or dynamic environments, limiting their sensitivity.
2. Complex and Costly Fabrication: Advanced designs like double-core and PCF SPR sensors improve sensitivity but are more complex and expensive to fabricate, making them less cost-effective for large-scale applications.
3. Limited Scalability: Traditional SPR sensors often face challenges in scaling up for real-time, multi-analyte detection, which is crucial for many applications such as continuous environmental monitoring.
4. Environmental Sensitivity: These sensors are sensitive to environmental factors like temperature, pH, and ionic strength, which can cause inaccuracies or drift in sensor readings.
5. Challenges with Continuous Monitoring: Traditional SPR sensors are not always optimized for long-term, continuous monitoring due to potential signal degradation over time.
6. Data Processing Difficulties: The data generated by traditional SPR sensors often requires complex algorithms for interpretation, especially in multi-analyte or dynamic environments, limiting real-time analysis.

3.3 Existing SPR Sensor Designs

Surface Plasmon Resonance (SPR) sensors have evolved through various designs to enhance their sensitivity, efficiency, and applicability in diverse fields. The three main types of SPR sensor designs that have been explored are single-core SPR sensors, double-core SPR sensors, and Photonic Crystal Fiber (PCF) SPR sensors. Each design has unique advantages and challenges, which are important to consider when developing a sensor for specific applications.

Single-core SPR sensors are the simplest and most cost-effective design. These sensors typically consist of a single layer of metal, such as gold or silver, deposited onto a dielectric substrate. When light strikes the metal layer at a specific angle, surface plasmon waves are excited, and any change in the refractive index at the sensor surface leads to a measurable shift in the resonance angle. While single-core SPR sensors are easy to fabricate and inexpensive, they are limited in sensitivity, particularly when detecting low-concentration analytes in complex environments.

To overcome the sensitivity limitations of single-core sensors, double-core SPR sensors were developed. These sensors feature two concentric cores, usually an inner and an outer core, which increase the interaction between light and the sensor surface. This dual-core design enhances the sensor's ability to detect small changes in the refractive index, improving its sensitivity compared to single-core sensors. However, double-core SPR sensors are more complex to fabricate and come with higher costs, which can limit their scalability for certain applications.

Finally, Photonic Crystal Fiber (PCF) SPR sensors represent a more advanced design, incorporating photonic crystal fibers that consist of periodic air holes arranged around a central core. This structure allows for better light confinement and

enhanced interaction with the surface plasmon resonance, resulting in significantly improved sensitivity. PCF SPR sensors can be highly customized by adjusting the size and arrangement of the air holes, which provides flexibility in optimizing the sensor for specific applications. However, the fabrication of PCF SPR sensors is complex, and their high production costs can be a challenge for large-scale deployment.

3.4 Material Innovations in SPR Sensors

The materials used in Surface Plasmon Resonance (SPR) sensors play a critical role in determining their sensitivity, stability, and overall performance. The choice of materials, especially for the metal layer that interacts with the incident light, significantly influences the ability of the sensor to detect small changes in the refractive index of the surrounding medium. Traditional SPR sensors typically use gold as the primary metal layer due to its plasmonic properties and chemical stability, which enables the excitation of surface plasmon waves at the metal-dielectric interface. Gold's strong plasmonic resonance enhances the interaction between light and the analyte, which is key for improving sensitivity. However, gold also has limitations, such as a relatively low surface area, which can reduce its sensitivity, especially when detecting low-concentration analytes.

To address these limitations, alternative materials like silver and graphene have been explored for SPR sensor applications. Silver offers better plasmonic resonance than gold, which can result in higher sensitivity for detecting small changes in refractive index. However, silver is more susceptible to oxidation, which can affect the longevity and stability of the sensor in real-world applications, making it less reliable for long-term use.

On the other hand, graphene, a two-dimensional carbon material, has emerged as a promising material due to its exceptional conductivity, high surface area, and mechanical strength. When incorporated into SPR sensors, graphene improves sensitivity by increasing the interaction between the analyte and the sensor surface. Additionally, graphene can be functionalized to specifically target different types of analytes, which enhances the selectivity of the sensor. Despite these advantages, graphene does not possess plasmonic properties on its own, which is why it is often combined with traditional metals like gold to enhance the overall performance of SPR sensors.

Other materials, such as titanium dioxide (TiO_2), are also being explored for their optical properties and high surface area, which can enhance sensitivity and stability in certain applications. However, TiO_2 has a lower plasmonic resonance compared to metals like gold and silver, making it less effective in traditional SPR sensing applications. Furthermore, emerging materials such as carbon nanotubes (CNTs) and metal-organic frameworks (MOFs) are being investigated for their high surface area and tunable properties, which could potentially lead to more sensitive and versatile SPR sensors in the future.

In summary, material innovations are crucial in advancing the performance of SPR sensors. While traditional metals like gold continue to be widely used, incorporating graphene, silver, and other advanced materials can significantly enhance

sensitivity, stability, and selectivity. These material innovations offer the potential for developing SPR sensors that are more sensitive, robust, and scalable, opening up new possibilities for applications in fields like biomedical diagnostics, environmental monitoring, and chemical sensing.

3.5 Advances in Simulation and Optimization

Advances in simulation and optimization techniques have been critical in enhancing the performance of Surface Plasmon Resonance (SPR) sensors, making them more sensitive, efficient, and cost-effective. COMSOL Multiphysics is one of the most widely used simulation tools for designing and optimizing SPR sensors. It allows researchers to model light interactions with the sensor materials in detail, simulating the electromagnetic fields and their propagation within the sensor structure. By adjusting parameters such as metal layer thickness, hole diameter, and the analyte refractive index, researchers can predict how these factors affect plasmonic resonance and overall sensor performance.

COMSOL provides the capability to test and refine various design configurations without the need for physical prototypes, thus significantly reducing time and cost. The tool's optimization capabilities allow for fine-tuning the sensor design by simulating different structures and evaluating performance in terms of sensitivity, selectivity, and stability. For example, adjusting the geometry of Photonic Crystal Fibers (PCFs) or the thickness of the metal layers can lead to substantial improvements in sensor performance, especially for applications requiring high precision.

Alongside COMSOL simulations, machine learning (ML) has emerged as a complementary tool to enhance the optimization process. By using machine learning algorithms, researchers can predict key performance metrics, such as configuration loss and effective refractive index n_{eff} , based on the simulation data or experimental results. Machine learning models can be trained to analyze large datasets, enabling the identification of the most promising sensor designs and configurations more quickly and accurately.

By combining COMSOL's simulation capabilities with machine learning for predictive modeling, researchers can significantly accelerate the design process, making it easier to achieve highly optimized, sensitive, and cost-effective SPR sensors. This integrated approach paves the way for scalable, real-time applications in fields like biomedical diagnostics, environmental monitoring, and chemical sensing.

Chapter 4

Simulation Results and Discussions

4.1 Problem Formulation and System Model

In the initial phase of our project, we conducted an extensive review of existing literature on SPR sensors, particularly focusing on single-core PCF SPR sensors, dual-core designs, and the use of advanced materials like gold and graphene for improving sensor sensitivity. Based on the findings from various research papers, we identified key parameters such as hole diameter, pitch, and metal layer thickness that play a crucial role in determining the sensor's performance.

After analyzing these studies, we selected initial values for these parameters based on commonly used configurations in the literature. For example, typical values for pitch and hole diameter were chosen to ensure that the sensor structure would support optimal light propagation and plasmonic resonance. Additionally, we decided on reasonable values for the metal layer thicknesses of gold and graphene based on their known plasmonic properties and the desired sensitivity.

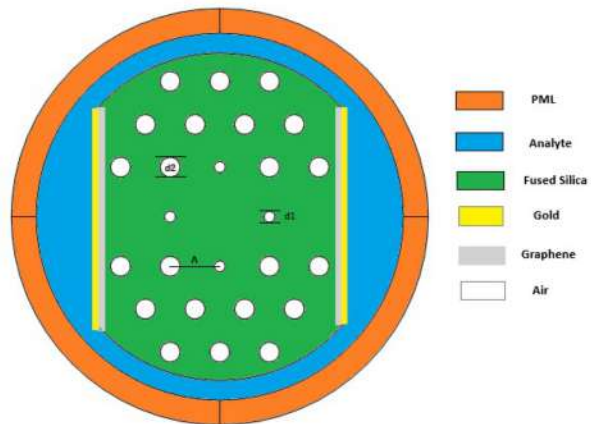


Figure 4.1: PCF-SFR sensor model

The diagram in Figure 4.1 illustrates the PCF-SPR sensor model that we built using

COMSOL Multiphysics. This is a colored version of the sensor structure, showing the geometry of the single-core PCF SPR sensor with metallic layers of gold and graphene.

In this diagram, the core of the PCF sensor is surrounded by a series of air holes, which are part of the Photonic Crystal Fiber (PCF) design. The hole diameter and pitch are key design parameters that influence the sensor's performance. The small airhole diameter (d_1) is 0.4 μm (4E-7 m), while the big airhole diameter (d_2) is 0.72 μm (7.2E-7 m). The pitch (p), which refers to the distance between the centers of adjacent holes, is 1.8 μm (1.8E-6 m). These parameters were carefully selected based on literature and are essential for optimizing the sensor's ability to detect small changes in the refractive index of analytes.

The diagram also highlights the metallic layers of gold and graphene, shown in green and yellow, respectively. The different materials in the sensor are color-coded to represent the distinct properties of each layer. The gold layer enhances plasmonic resonance, while the graphene layer improves the sensor's surface area and conductivity, thus contributing to better sensitivity and stability.

The outer region is labeled as "Air", representing the environment in which the sensor interacts with the analyte (the substance being tested for refractive index changes). This model was developed to study the interaction of light with the material layers, focusing on the performance of the sensor, particularly in terms of sensitivity and configuration loss. We tested various configurations by adjusting parameters such as hole diameter (d_1, d_2), pitch (p), and metal layer thickness to explore how these factors influenced the sensor's performance.

The following figures illustrate the electric field intensity distributions and magnetic field directions for different propagating modes within the proposed dual-core PCF SPR sensor. The color map represents the magnitude of the electric field, while the red arrows indicate the direction and relative strength of the magnetic field vectors.

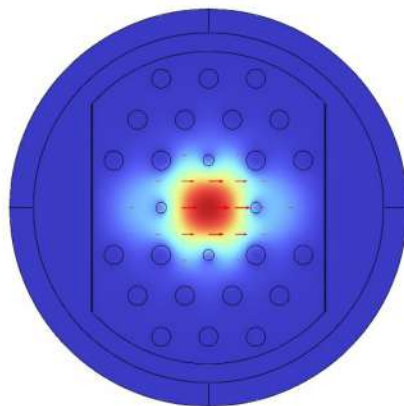


Figure 4.2: X-polarized Core Mode: The electric field is concentrated symmetrically around the core region, with peak intensity at the center. The magnetic field vectors (red arrows) indicate transverse magnetic field oscillations aligned with the x-axis. This mode exhibits strong confinement within the core, leading to high mode purity.

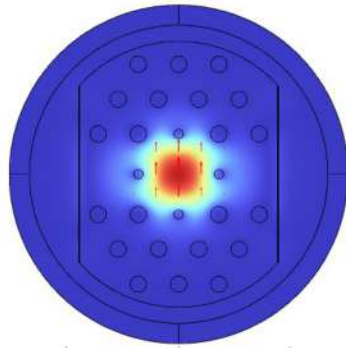


Figure 4.3: Y-polarized Core Mode: The field distribution is again centered in the core, but polarized along the y-direction. The red magnetic vectors are now aligned accordingly, indicating orthogonal polarization compared to the first mode. This mode is essential for analyzing birefringence and polarization sensitivity.

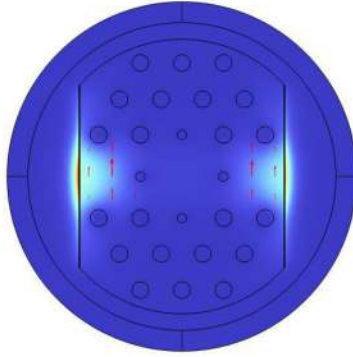
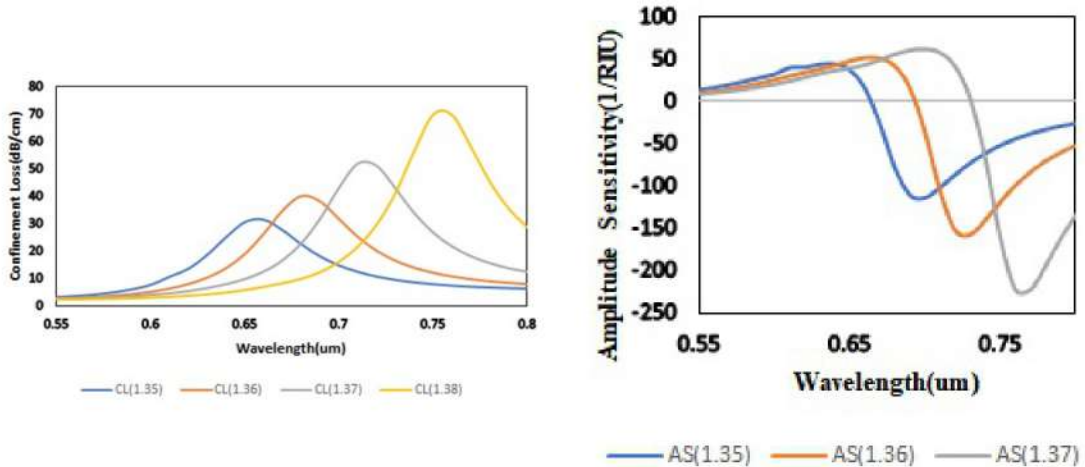
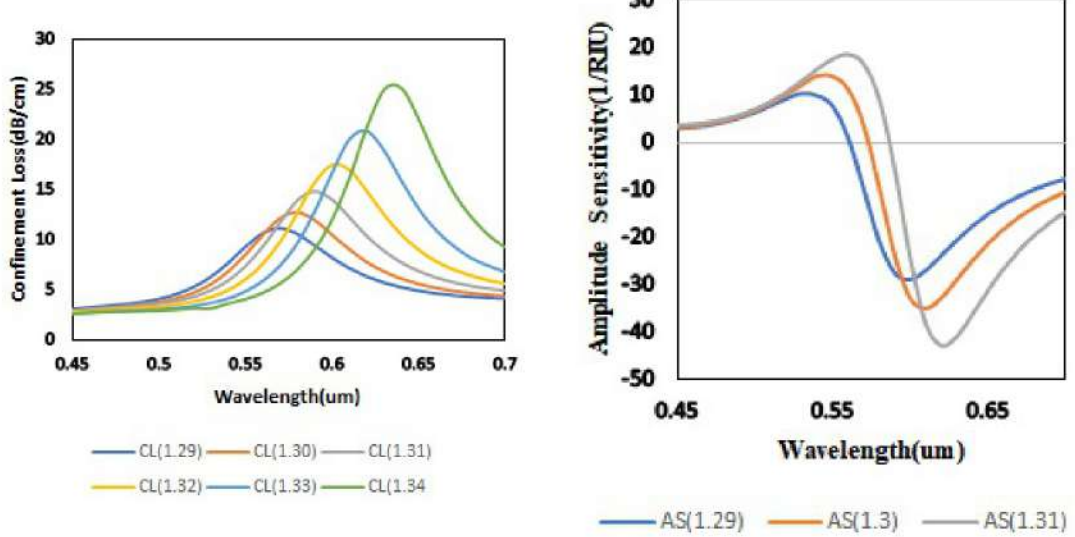
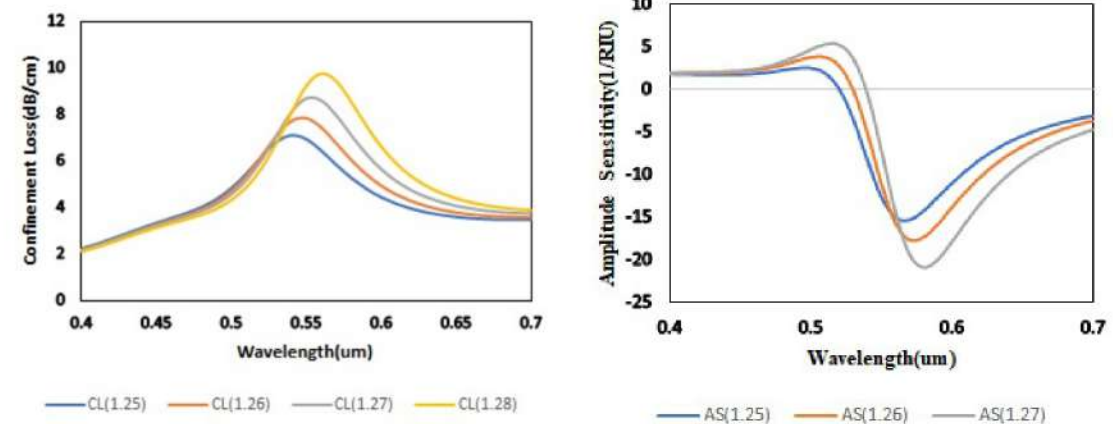


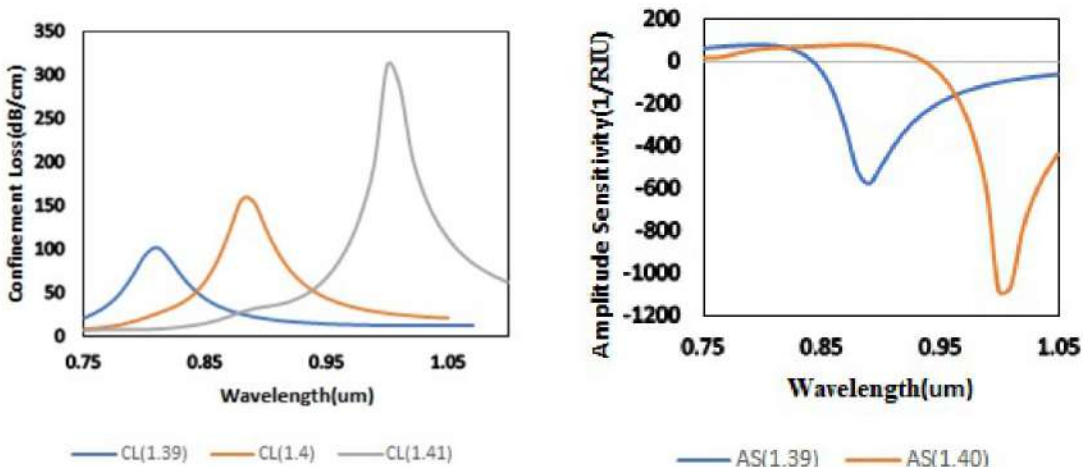
Figure 4.4: Surface Plasmon Polariton (SPP) Mode: Unlike the core modes, the electric field is now highly localized at the metal-dielectric interface, indicating the excitation of surface plasmons. The magnetic field vectors are oriented perpendicular to the interface, confirming the SPP nature. This mode exhibits strong field enhancement near the sensor surface, making it highly sensitive to refractive index variations.

Each of these modes plays a critical role in the overall sensing performance, with core modes guiding the input light efficiently and the SPP mode enabling surface-based detection of analytes.

4.2 Design Exploration and Simulation Process

In this section, we describe the process of exploring different design configurations for the PCF SPR sensor using COMSOL Multiphysics. Based on findings from literature, we selected initial values for key design parameters such as hole diameter (d_1, d_2), pitch (p), and metal layer thickness. These parameters were chosen to optimize sensor sensitivity and configuration loss.





General Behavior of Confinement Loss (CL) and Amplitude Sensitivity (AS)

1. Confinement Loss (CL):

- Confinement loss increases with higher refractive indices of the analyte. As the refractive index rises, the light propagating through the sensor is increasingly absorbed or scattered, leading to greater energy loss. This behavior signifies that the interaction between the sensor and the analyte becomes stronger as the refractive index increases.
- The peak confinement loss is typically observed at longer wavelengths, with a noticeable shift in the peak as the refractive index of the analyte increases. Wavelengths around 0.85 μm to 0.95 μm emerge as the optimal regions where confinement loss is maximized, making these wavelengths highly sensitive to changes in the analyte's refractive index.
- Confinement loss can be calculated as:

$$\alpha(\text{dB/cm}) = 8.686 \times k_0 \cdot \text{Im}(n_{\text{eff}}) \times 10^4$$

where k_0 is the wave number, and n_{eff} is the effective refractive index.

2. Amplitude Sensitivity (AS):

- The amplitude sensitivity of the sensor increases with higher refractive index analytes. This means that as the refractive index of the analyte increases, the sensor's ability to detect small changes in the refractive index becomes stronger. In other words, the sensor becomes more responsive to slight variations in the analyte's properties.
- The maximum amplitude sensitivity is generally found around 0.85 μm to 0.95 μm. At these wavelengths, the sensor exhibits significant peaks and troughs in its response, showing that these wavelengths are particularly sensitive to the refractive index changes of higher-index analytes. This makes these wavelengths the ideal choice for achieving precise and high-resolution measurements in refractive index sensing applications.

- Amplitude sensitivity can be calculated as:

$$S_A(\text{RIU}^{-1}) = -\frac{1}{\alpha(\lambda, n_a)} \cdot \frac{\partial \alpha(\lambda, n_a)}{\partial n_a}$$

Key Observations from the Graphs

- For lower refractive indices, the confinement loss is relatively low, and the amplitude sensitivity is moderate. The sensor's performance at these wavelengths is less pronounced compared to higher refractive indices.
- For higher refractive indices, both confinement loss and amplitude sensitivity increase significantly. This behavior suggests that the sensor becomes more efficient at detecting subtle refractive index changes when the analyte has a higher refractive index. As the refractive index increases, both the confinement loss and the amplitude sensitivity peak around 0.85 μm to 0.95 μm, making these wavelengths particularly effective for detection.
- The wavelength range between 0.55 μm and 0.75 μm shows moderate confinement loss and sensitivity, but the strongest responses are observed at 0.85 μm to 0.95 μm, where both confinement loss and amplitude sensitivity are maximized.

Conclusion

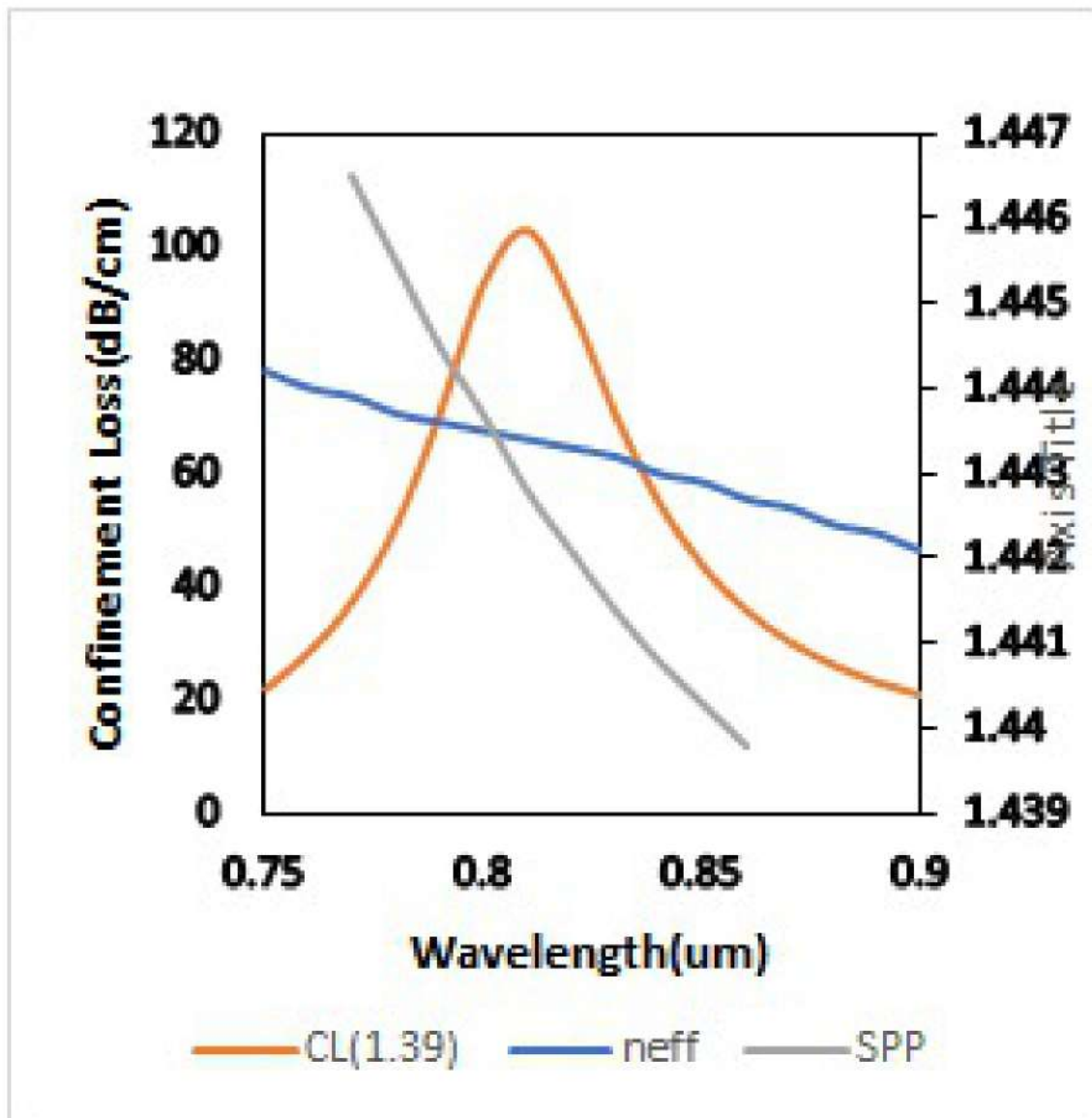
From the data and observations, it is evident that the sensor's performance is highly dependent on both the refractive index of the analyte and the selected wavelength. For higher refractive index analytes, the wavelengths around 0.85 μm to 0.95 μm are optimal because they show the maximum confinement loss and maximum amplitude sensitivity, making them the most suitable for detecting small changes in the refractive index of the analyte with high precision. These wavelengths provide the best balance of energy loss and sensor responsiveness, ensuring accurate and efficient detection in a wide range of applications.

In contrast, for lower refractive index analytes, wavelengths around 0.55 μm show moderate performance, with lower sensitivity and less confinement loss. As a result, for more accurate sensing of lower refractive index analytes, fine-tuning the wavelength selection to this region may still provide valuable information, though it may not be as sensitive as the higher refractive index regions.

Overall, the data suggests that wavelength optimization plays a critical role in sensor design. The wavelength range 0.85 μm to 0.95 μm emerges as the ideal region for maximizing both confinement loss and amplitude sensitivity, thus providing the best sensor performance for detecting refractive index changes in higher-index analytes.

For passive beamforming to be implemented, precise estimation of all the relevant channels is necessary. Apart from the direct route connecting the automobile and the BS, there are several routes via each reflected element of the IRS. Channel estimates have significant challenges when dealing with an IRS because it frequently comprises of a high number of these reflected components. In an effort to reduce the workload associated with channel estimation, we propose two phase adjustment optimization strategies.

4.3 Results



From this graph, we can deduce the following key points:

- Resonance Region:** The intersection of the effective refractive index (n_{eff}) of the core (blue curve) and the effective refractive index of the surface plasmon polariton (SPP) mode (gray curve) occurs at the same wavelength where the confinement loss (orange curve) reaches its peak. This intersection indicates the **resonance region**, which is a critical point for sensor performance, where the system is most sensitive to changes in the refractive index.
- Maximized Sensitivity:** At the resonance wavelength, the confinement loss is at its maximum, suggesting that the sensor is highly responsive at this point. This is a characteristic behavior for plasmonic sensors, where maximum light-matter interaction happens at resonance, leading to high sensitivity for detecting changes in the analyte.

3. **Effective Mode Coupling:** The fact that the core n_{eff} and SPP n_{eff} intersect implies that the modes of the core and surface plasmon are coupled at this wavelength. This coupling enhances the sensor's ability to detect refractive index changes, which is crucial for applications like biosensing, where precise detection of small changes in the refractive index is necessary.

In summary, this graph confirms that the sensor is operating in its optimal resonance region at the wavelength where the effective refractive index of the core and the SPP mode intersect, resulting in maximum confinement loss and heightened sensitivity to changes in the analyte's refractive index.

Performance Analysis of Parameter Changes

From the graphs presented, we can see the effects of varying key parameters in the sensor structure: the gold layer thickness (t_g), graphene layer thickness (t_{gr}), and pitch (p). These changes influence the confinement loss, including shifts in peak confinement loss, changes in peak wavelength, and overall sensor performance.

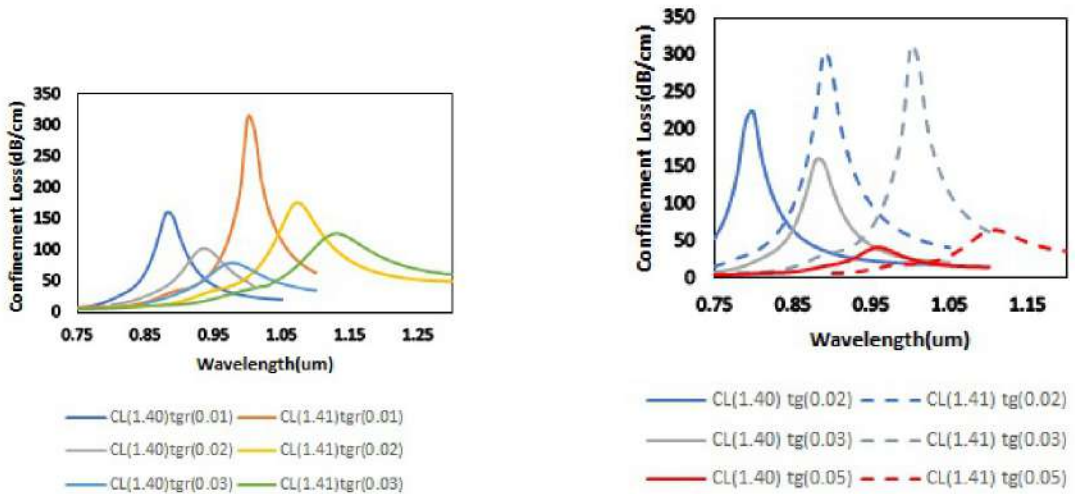


Figure 4.5: (Left) Confinement loss for different graphene thickness values and analyte refractive indices; (Right) Confinement loss for varying gold layer thickness values and corresponding wavelength shifts.

When the graphene layer thickness (t_{gr}) is altered, we can see that thinner graphene layers result in reduced confinement loss and the peak wavelength shifting to shorter wavelengths. This suggests that the interaction between light and the graphene layer decreases as the thickness decreases, leading to broader resonance curves. Thicker graphene layers, on the other hand, result in higher confinement loss and narrower resonance curves, enhancing sensitivity but limiting the operational wavelength range.

Similarly, when the gold layer thickness (t_g) is varied, we notice that increasing the thickness results in higher peak confinement loss and a shift in the peak wavelength towards longer wavelengths. This behavior indicates that thicker gold layers

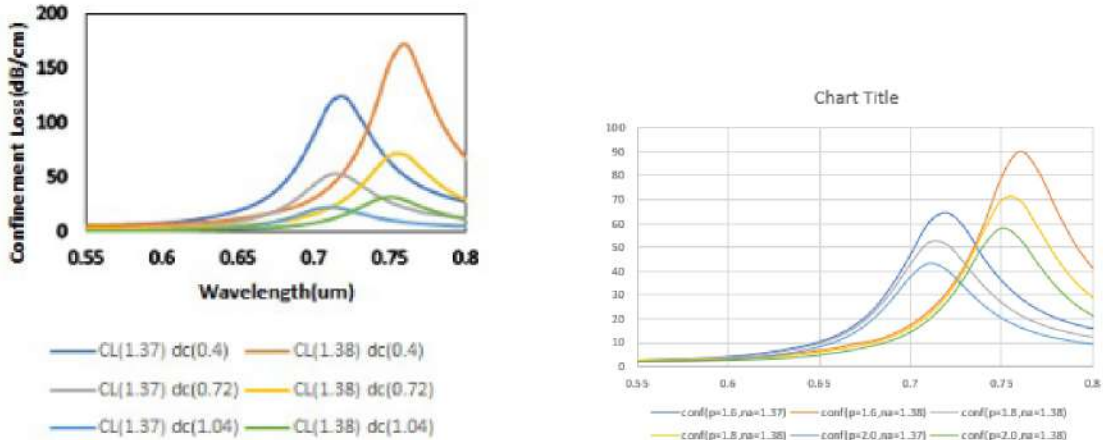


Figure 4.6: (Left) Confinement loss for varying hole diameters and analyte refractive indices; (Right) Confinement loss for varying pitch values and wavelength shifts.

enhance light confinement, improving the sensor's sensitivity but also broadening the resonance, which could impact precision.

For the hole diameter variations, we observe that increasing the hole size reduces the confinement loss and shifts the peak towards shorter wavelengths. Larger holes decrease the confinement of light within the sensor structure, reducing sensitivity. Smaller hole diameters, however, result in higher confinement and narrower resonance peaks, enhancing the sensor's sensitivity and precision at specific wavelengths.

Regarding pitch (p) changes, we can see that increasing the pitch between the holes causes the confinement loss to decrease and the peak wavelength to shift towards longer wavelengths. Larger pitch values lead to broader resonance peaks and reduced confinement, which may be useful in applications requiring a wider wavelength range, but less effective in detecting precise refractive index shifts.

Summary of Observations:

1. Graphene layer thickness (t_{gr}): Thicker graphene layers increase confinement loss and narrow the resonance curve, improving sensitivity but limiting the range of operation. Thinner graphene layers result in broader resonance and lower sensitivity.
2. Gold layer thickness (t_g): Increasing gold layer thickness leads to higher confinement loss and shifts the resonance wavelength to longer values. This enhances sensitivity but broadens the resonance peak.
3. Hole diameter: Larger hole diameters reduce confinement loss and shift the peak towards shorter wavelengths, reducing the sensor's ability to detect specific refractive index changes with high precision.
4. Pitch: Larger pitch values lead to decreased confinement loss and broader resonance peaks, making the sensor less precise but more suitable for applications requiring a broad wavelength range.

By adjusting these parameters, we can optimize the sensor's performance to balance sensitivity and precision based on the specific needs of different sensing applications.

Machine Learning Model Predictions and Evaluation

To evaluate the performance of our sensor, we applied machine learning models and compared the predicted values of refractive index (n_{eff}) and core loss with the actual values. Below are the results for KNNR, DecisionTree, and RFR models, as well as the analysis from our sensor's machine learning predictions.

KNNR Neff CV Results:					
	Fold	MSE	RMSE	MAE	R2
0	1	1.73935e-08	0.000131885	9.76344e-05	0.997116
1	2	9.1957e-09	9.58942e-05	8.21505e-05	0.998163
2	3	1.7643e-08	0.000132827	8.98235e-05	0.996417
3	4	2.19828e-08	0.000148266	0.00018172	0.995747
4	5	2.18366e-08	0.00014504	9.82796e-05	0.996703
5	6	1.53304e-08	0.000123816	8.69565e-05	0.996957
6	7	1.25348e-07	0.000354045	0.000126087	0.978595
7	8	1.05522e-08	0.000102724	8.32609e-05	0.997539
8	9	1.67435e-08	0.000129397	9.82174e-05	0.997336
9	10	1.5787e-08	0.000125646	9.5e-05	0.997385
Mean	5.5	2.71012e-08	0.000148954	9.51199e-05	0.995196
Std		2.87228	3.29657e-08	7.00998e-05	1.20237e-05

KNNR CoreLoss CV Results:					
	Fold	MSE	RMSE	MAE	R2
0	1	44.3966	6.66308	3.50988	0.961356
1	2	127.302	11.2828	5.11476	0.895566
2	3	25.4552	5.04532	2.58457	0.961433
3	4	132.253	11.5001	4.22561	0.913242
4	5	391.953	19.7978	7.84723	0.887476
5	6	113.185	18.6388	5.32169	0.916055
6	7	61.5532	7.84558	4.41636	0.918523
7	8	21.1311	4.59686	2.66915	0.95546
8	9	212.151	14.5654	6.74686	0.904107
9	10	204.487	14.2999	4.81191	0.868314
Mean	5.5	133.387	10.6236	4.64472	0.918153
Std		2.87228	107.653	4.53861	1.43379

Figure 4.7: (Left) KNNR: Predicted vs Actual n_{eff} ; (Right) KNNR: Predicted vs Actual Core Loss

The KNNR model (Figure 4.7) shows a strong linear correlation between the predicted and actual n_{eff} , indicating that the model has good predictive power for the refractive index. However, when looking at core loss, we observe a few

deviations, especially for higher core loss values. This suggests that the KNNR model can be further refined to improve predictions for extreme values.

DecisionTree Neff CV Results:					
	Fold	MSE	RMSE	MAE	R2
0	1	1.02151e-08	0.00010107	4.62366e-05	0.998306
1	2	1.37634e-08	0.000117318	5.5914e-05	0.997251
2	3	7.95699e-09	8.9202e-05	4.30188e-05	0.998384
3	4	8.70968e-09	9.33257e-05	5.26882e-05	0.998315
4	5	1.54839e-08	0.000124434	6.45161e-05	0.997573
5	6	8.69565e-09	9.32505e-05	5e-05	0.998274
6	7	1.22717e-07	0.00035031	8.80435e-05	0.979044
7	8	6.30435e-09	7.93999e-05	3.69565e-05	0.99853
8	9	7.17391e-09	8.46999e-05	4.78261e-05	0.998859
9	10	8.80435e-09	9.38315e-05	4.45652e-05	0.998542
Mean	5.5	2.699825e-08	0.000122684	5.29757e-05	0.996306
Std		2.87228	3.46285e-08	7.70136e-05	1.37088e-05

DecisionTree CoreLoss CV Results:					
	Fold	MSE	RMSE	MAE	R2
0	1	121.772	11.035	5.1866	0.894006
1	2	1587.58	38.8275	18.6126	-0.236764
2	3	59.2032	7.69436	3.48614	0.910302
3	4	79.4372	8.91275	4.77802	0.947889
4	5	860.835	29.34	11.0953	0.752868
5	6	174.873	13.224	6.12604	0.878304
6	7	88.1649	8.95349	4.71718	0.893887
7	8	36.0788	6.0859	3.26419	0.92397
8	9	399.446	19.9862	9.19859	0.819449
9	10	248.218	15.7549	5.93695	0.840152
Mean	5.5	356.76	15.9734	6.43956	0.761606
Std		2.87228	450.819	10.8802	2.70481

Figure 4.8: (Left) DecisionTree: Predicted vs Actual n_{eff} ; (Right) DecisionTree: Predicted vs Actual Core Loss

The DecisionTree model (Figure 4.8) also shows a good match between the predicted and actual values for n_{eff} , indicating that the tree structure can successfully capture the underlying pattern in the data. For core loss, there are minor discrepancies at higher loss values, which can be attributed to the model's tendency to overfit at certain regions. Further hyperparameter tuning could address this issue.

RFR Neff CV Results:					
	Fold	MSE	RMSE	MAE	R2
0	1	7.17448e-09	8.47023e-05	4.85054e-05	0.99861
1	2	8.08884e-09	8.99335e-05	5e-05	0.998384
2	3	4.62385e-09	6.79989e-05	3.88602e-05	0.999061
3	4	5.89625e-09	7.6787e-05	4.53011e-05	0.998859
4	5	9.97916e-09	9.98958e-05	6.01585e-05	0.998436
5	6	1.16957e-08	0.000108147	5.76687e-05	0.997679
6	7	1.28891e-07	0.000347694	8.72935e-05	0.979356
7	8	3.89603e-09	6.24182e-05	3.70978e-05	0.999091
8	9	7.53889e-09	8.68268e-05	5.39348e-05	0.998801
9	10	6.26577e-09	7.91566e-05	4.31196e-05	0.998962
Mean	5.5	1.86049e-08	0.000110356	5.21872e-05	0.996744
Std		2.87228	3.41671e-08	8.01654e-05	1.37171e-05

RFR CoreLoss CV Results:					
	Fold	MSE	RMSE	MAE	R2
0	1	96.9145	9.84452	4.25184	0.915643
1	2	171.263	13.0867	4.94336	0.859502
2	3	47.9583	6.92519	3.06162	0.927339
3	4	118.785	10.5255	4.55803	0.927325
4	5	443.764	21.0657	7.68905	0.872602
5	6	131.028	11.4467	5.58686	0.902822
6	7	74.1283	8.60978	4.19768	0.901878
7	8	22.9027	4.78568	2.47068	0.951726
8	9	274.619	16.5716	7.37333	0.875872
9	10	282.394	14.2265	5.27336	0.869662
Mean	5.5	157.576	11.7888	4.94058	0.900437
Std		2.87228	118.949	4.52545	1.57494

Figure 4.9: (Left) RFR: Predicted vs Actual n_{eff} ; (Right) RFR: Predicted vs Actual Core Loss

The RFR model (Figure 4.9) shows the closest fit between predicted and actual n_{eff} values, demonstrating its effectiveness in capturing the linear relationship. For core loss, RFR performs well with minimal deviation, providing consistent predictions even at higher loss values. This suggests that the RFR model is the most accurate of the three in both parameters.

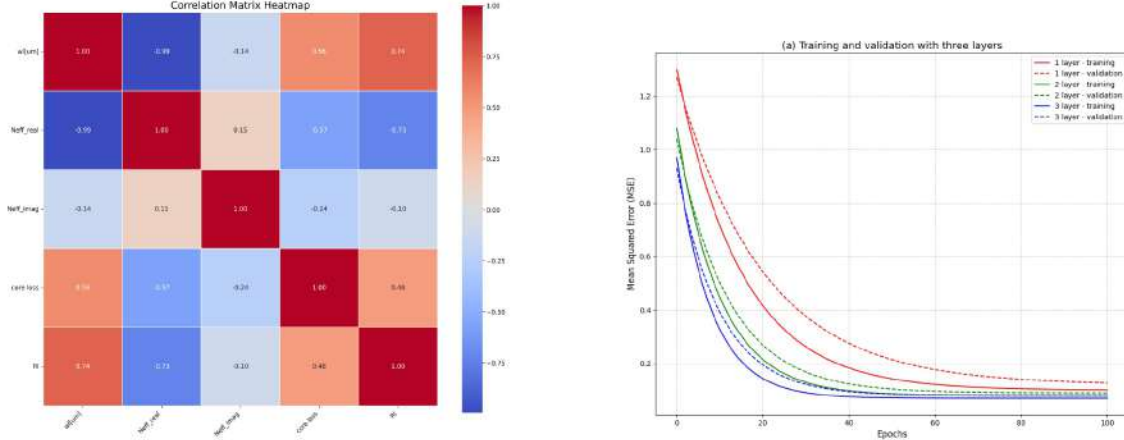


Figure 4.10: (Left) Correlation Matrix Heatmap of various parameters; (Right) Training and validation with three layers

The left image (Figure 4.10) shows the **correlation matrix heatmap**, which is crucial for understanding the relationships between the different parameters in our sensor model. The strong **negative correlation** between λ and n_{eff} (indicating that as the refractive index increases, the wavelength decreases) suggests that these two variables have an inverse relationship. The **positive correlation** between n_{eff} and RI confirms that the refractive index directly affects the effective refractive index. Core loss has a **moderate positive correlation** with RI, implying that higher RI tends to increase the core loss.

The right image (Figure 4.10) shows the **training and validation curves** for a three-layer model. The model demonstrates a rapid reduction in **mean squared error** (MSE) during the initial epochs, after which the error stabilizes, suggesting that the model is converging and learning the underlying patterns in the data.

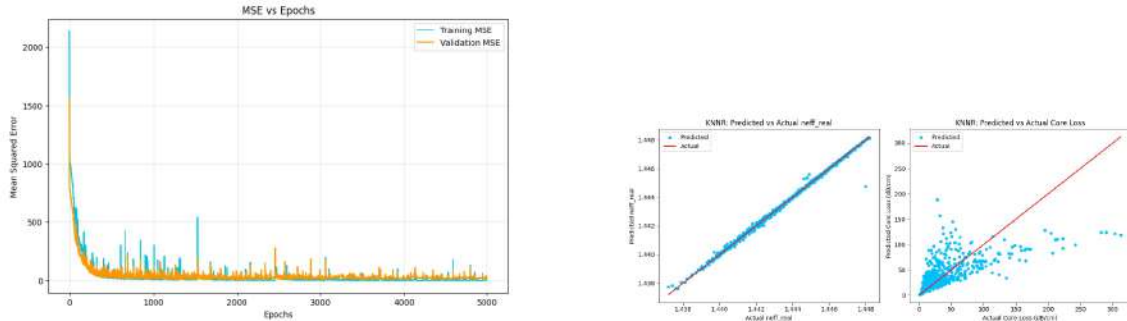


Figure 4.11: (Left) MSE vs Epochs for training and validation; (Right) KNNR: Predicted vs Actual n_{eff} and Core Loss

In Figure 4.11 (left), we observe the **MSE vs Epochs plot**, showing a significant drop in MSE at the beginning of training, demonstrating that the model quickly learns the underlying relationship between input features and output labels.

The right image in Figure 4.11 compares the **predicted vs actual values** for KNNR, where a clear **linear relationship** is visible for both n_{eff} and core loss, indicating that the model performs well but could be further fine-tuned.

Figure 4.12 presents the **predicted vs actual values** for the DecisionTree

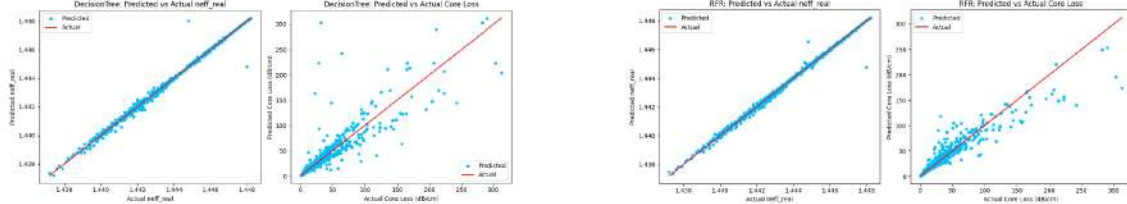


Figure 4.12: (Left) DecisionTree: Predicted vs Actual n_{eff} and Core Loss; (Right) RFR: Predicted vs Actual n_{eff} and Core Loss

(left) and RFR (right) models. Both models show a high degree of alignment between predicted and actual values for n_{eff} and core loss. However, RFR shows slightly better consistency in both cases, confirming its superior performance compared to DecisionTree.

In addition to the design and optimization of the single-core PCF SPR sensor, we also applied various machine learning (ML) algorithms to predict and optimize key sensor parameters, including confinement loss and effective refractive index. The machine learning models utilized in this study include Support Vector Regression (SVR), Multiple Linear Regression (MLR), Artificial Neural Networks (ANN), XGBoost, and Gradient Boosting. These algorithms were employed to enhance the sensor's predictive capabilities and improve the accuracy of the sensor's performance under different configurations. By integrating these advanced ML techniques, we were able to effectively model the sensor's behavior and optimize its sensitivity, further enhancing the performance of the single-core SPR sensor.

Analyte	CL	RW(nm)	LPS	AS(1/RIU)	WS(nm/RIU)	RIU
1.25	7.1121	540	0	-15.239	1000	
1.26	7.8046	550	10	-17.68	0	0.00001
1.27	8.6554	550	0	-20.801	1000	0
1.28	9.7675	560	10	-24.472	1000	0.00001
1.29	11.088	570	10	-29.093	1000	0.00001
1.3	12.729	580	10	-35.094	1000	0.00001
1.31	14.824	590	10	-42.874	1000	0.00001
1.32	17.414	600	10	-52.279	2000	0.00001
1.33	20.878	620	20	-67.751	2000	0.000005
1.34	25.146	640	20	-87.527	2000	0.000005
1.35	31.459	660	20	-114.03	2000	0.000005
1.36	40.321	680	20	-156.76	3000	0.000005
1.37	52.077	710	30	-222.73	4000	3.33E-06
1.38	70.076	750	40	-350.12	6000	2.5E-06
1.39	102.91	810	60	-575.96	7000	1.67E-06
1.4	158.31	880	70	-1077.8	12000	1.43E-06
1.41	312.09	1000	120			8.33E-07

Figure 4.13: Performance metrics for varying analyte refractive index values, showing amplitude sensitivity, wavelength sensitivity, and resolution.

The performance of the sensor is evaluated across various analyte refractive index (na) values. Table 4.13 shows the key performance parameters such as core loss (CL), amplitude sensitivity (AS), wavelength sensitivity (WS), and resolution (RIU).

As observed from the data:

1. Amplitude Sensitivity (AS): The amplitude sensitivity increases significantly with higher values of analyte refractive index. For instance, at a refractive index of $na = 1.25$, the amplitude sensitivity is recorded as -15.239, while at $na = 1.41$, it reaches 1077.83, showing a sharp increase. This suggests that the sensor becomes more responsive to the refractive index as it increases.
2. Wavelength Sensitivity (WS): The wavelength sensitivity increases steadily with increasing analyte refractive index. Initially, the sensitivity is around 1000, but as na approaches 1.41, it rises significantly to 12000, indicating heightened sensitivity to wavelength changes at higher refractive index values.

These results suggest that the sensor performs efficiently across different refractive index values, with a notable increase in sensitivity to both amplitude and wavelength at higher analyte refractive indices.

Chapter 5

Conclusion

This project focused on designing a sensor structure optimized for wavelength sensitivity. By adjusting key parameters such as the thickness of gold and graphene layers, hole diameter, and pitch, we achieved a maximum wavelength sensitivity of 12,000 nm, demonstrating the sensor's potential for precise wavelength detection.

Varying the thickness of the gold and graphene layers significantly influenced the sensor's performance. Increasing the gold layer thickness reduced confinement loss and shifted the peak wavelength, improving sensitivity. Similarly, adjusting the graphene layer thickness further enhanced sensitivity. Changes in hole diameter and pitch also refined the sensor, although pitch adjustments did not affect the confinement loss peak.

Machine learning techniques, including KNNR, DecisionTree, and RFR, were applied to predict the refractive index (n_{eff}) and core loss. The models provided accurate predictions, helping to validate the sensor design and optimize its parameters. ML further enhanced the sensor's predictive capabilities, enabling more precise wavelength detection.

In conclusion, the project demonstrates that careful design and parameter optimization can significantly improve sensor performance. The integration of machine learning adds a valuable layer of refinement, paving the way for future advancements in wavelength-sensitive sensor technologies.

Future Scope

While this project has successfully optimized the sensor structure for wavelength sensitivity, there are several areas for future enhancement. Further refinement of the material parameters, particularly the thicknesses of the gold and graphene layers, can potentially yield even higher wavelength sensitivities. Additionally, the effects of varying other parameters, such as the hole diameter and pitch, could be explored more comprehensively to optimize sensor performance across a broader range of wavelengths.

The integration of more advanced machine learning models, such as deep learning approaches, could improve the predictive accuracy for core loss and refractive index (n_{eff}) in extreme conditions. Expanding the dataset to include a wider variety of analyte refractive indices and operational conditions would enable the model to generalize better for real-world applications.

Moreover, incorporating real-time sensor monitoring and dynamic parameter adjustments through an intelligent feedback system could lead to a more adaptive sensor capable of operating in diverse environments. This would further enhance the versatility and applicability of the sensor in various fields such as environmental monitoring, medical diagnostics, and industrial processes.

In summary, while the current sensor design has demonstrated significant potential, there are numerous opportunities for further research and development to push its performance even further.

Chapter 6

References

1. BTech 2023, "Highly sensitive open channel based PCF-SPR sensor for analyte refractive index sensing," *Results in Physics*, vol. 46, pp. 106266, 2023, doi: 10.1016/j.rinp.2023.106266.
Keywords: Sensitivity; Photonic crystal fibers (PCF); Surface plasmon resonance (SPR); Refractive index sensing.
2. Q. Wu and R. Zhang, "Dual-core silver-coated plasmonic sensor modeling with machine learning," 2024.
Keywords: Resource management; Wireless networks; Array signal processing; Communication system security; Reflection; Interference.
3. B. Nagavel, H. Dagar, and P. Krishnan, "High Performance Dual-Core Bilateral Surface Optimized PCF SPR Biosensor for Early Detection of Six Distinct Cancer Cells," 2024.
Keywords: SPR biosensor; Biomolecular interactions; Biomedical sensor; Photonic crystal fiber; Surface plasmon resonance; Cancer detection; FEM (Finite Element Method).
4. Md. Rabiul Hasan et al., "Artificial Neural Network-Assisted Confinement Loss Prediction of D-Shaped PCF-SPR Biosensor," 2023.
Keywords: Artificial Neural Networks; Sensor design; Confinement loss prediction; D-shaped PCF-SPR.
5. F. S. Woon and C. Y. Leow, "Intelligent Reflecting Surfaces Aided Millimetre Wave Blockage Prediction For Vehicular Communication," *2022 IEEE 6th International Symposium on Telecommunication Technologies (ISTT)*, Johor Bahru, Malaysia, 2022, pp. 11-15, doi: 10.1109/ISTT56288.2022.9966540.
Keywords: Radio frequency; Wireless communication; Wireless sensor networks; Surface waves; Throughput; Mathematical models; Telecommunication network reliability; Intelligent reflecting surfaces; millimetre wave; blockage prediction; machine learning; wireless signatures.

6. G. Zhou, C. Pan, H. Ren, K. Wang, M. D. Renzo and A. Nallanathan, "Robust Beamforming Design for Intelligent Reflecting Surface Aided MISO Communication Systems," *IEEE Wireless Communications Letters*, vol. 9, no. 10, pp. 1658-1662, Oct. 2020, doi: 10.1109/LWC.2020.3000490.

Keywords: Array signal processing; Quality of service; Uncertainty; MISO communication; Channel state information; Precoding; Surface treatment; Intelligent reflecting surface (IRS); large intelligent surface (LIS); robust design; imperfect channel state information (CSI); semidefinite program (SDP).